ACCSCIENCE PUBLISHING

Advances in Radiotherapy & Nuclear Medicine

ORIGINAL RESEARCH ARTICLE

Renal function reconstruction and modeling in dynamic scintigraphy

Faycal Kharfi[1]*, Haithem Aloui[2], and Rabie Benlabga[2]

[1]Laboratory of Dosing, Analysis, and Characterization with High Resolution, Department of Physics, Faculty of Sciences, Ferhat Abbas University Setif 1, Setif, Setif, Algeria

[2]Service of Nuclear Medicine, Babors Medical Clinic, Setif, Setif, Algeria

Abstract

Dynamic renal scintigraphy is a key imaging technique for assessing renal function using time-activity curves (TACs), which represent radiotracer uptake and clearance. TAC accuracy depends on the region of interest (ROI) selection and the modeling approach used. This study aims to: (i) Reconstruct TACs manually using gray-level values in scintigraphic images and compare them to machine-generated TACs using key kinetic parameters (T_{max}, $T_{1/2}$, and the 30-min min/max ratio); and (ii) evaluate the effectiveness of a one-compartment empirical mathematical model for TAC fitting and its physiological relevance. Twelve clinical cases were analyzed, with TACs reconstructed manually using a rectangular ROI selection method and compared to those automatically generated by the scintigraphy machine. An empirical mathematical fitting function was developed to improve TAC fitting. Manually reconstructed TACs showed better dynamic behavior and physiological accuracy over machine-generated TACs, particularly due to differences in ROI selection and signal processing. Using gray-level values instead of raw radioactive counts enhanced the depiction of kidney dynamics. The proposed mathematical model demonstrated a strong correlation (R^2 close to 1) and low error metrics, confirming its suitability for renal function assessment. While a free-hand ROI selection may improve accuracy, the rectangular method gives valuable results for the considered cases. This study highlights the importance of ROI selection in TAC reconstruction and demonstrates how manual methods and mathematical modeling can enhance renal functional assessment in clinical practice. Future work should validate these findings in larger datasets and assess the reproducibility of the proposed approach across different patient populations and imaging systems.

Keywords: Dynamic renal scintigraphy; Time-activity curve; Kinetic parameters; Mathematical modeling; Renal function assessment

***Corresponding author:**
Faycal Kharfi
(kharfifaycal@univ-setif.dz)

Citation: Kharfi F, Aloui H, Benlabga R. Renal function reconstruction and modeling in dynamic scintigraphy. *Adv Radiother Nucl Med.* 2025;3(2):61-72.
doi: 10.36922/ARNM025070008

Received: February 15, 2025

Revised: March 14, 2025

Accepted: April 21, 2025

Published online: May 6, 2025

1. Introduction

Dynamic renal scintigraphy is a diagnostic imaging technique used to assess the function and blood flow of the kidneys. It involves injecting a small amount of radioactive tracer, usually technetium-99m diethylene triamine penta-acetic acid or technetium-99m mercaptoacetyltriglycine (MAG3), into the bloodstream. As the radioactive tracer circulates through the bloodstream, it is filtered by the kidneys and excreted into the

urine. A gamma camera is used to detect the radiation emitted by the tracer, allowing the visualization of the kidneys and the urinary system in real time. Dynamic renal scintigraphy provides valuable information about renal function, including glomerular filtration rate (GFR), renal blood flow, and tubular function. It is commonly used in renal function evaluation, renal transplant assessment, and various kidney disorder diagnoses, such as hydronephrosis, renal obstruction, and renal artery stenosis. The "dynamic" aspect of the procedure refers to the continuous imaging of the kidneys over a period of time, typically several minutes, allowing clinicians to observe the tracer's movement through the renal system and assess kidney function dynamically. This dynamic imaging is often accompanied by static images taken at specific time points to provide additional information.

Renal function modeling in dynamic scintigraphy uses mathematical algorithms to analyze imaging data and assess renal function. This allows a more comprehensive assessment of renal function beyond simple visual observation. The typical steps for renal function reconstruction and modeling are:

(i) Data acquisition: Dynamic renal scintigraphy involves acquiring a series of images over time as the radioactive tracer circulates through the kidneys. These images are typically obtained using a gamma camera.
(ii) Image processing: The acquired images are processed to correct for factors such as background noise, scatter, and attenuation. This ensures the accuracy of the data used for analysis.
(iii) Region of interest (ROI) selection: ROIs are delineated on the images to isolate the kidneys and other relevant structures, such as the bladder and blood vessels.
(iv) Time-activity curve (TAC) generation: The intensity of the radioactive tracer within the kidneys is measured over time to create TACs. These curves represent the uptake, distribution, and clearance of the tracer within the kidneys.[1]
(v) Renal function parameters: Various parameters can be derived from the TACs to assess renal function, including:
    - GFR: GFR is a key indicator of renal function and can be estimated from the rate of tracer clearance from the blood.
    - Renal blood flow: The perfusion of blood through the kidneys can be estimated from the initial uptake and distribution of the tracer.
    - Tubular function: Parameters such as tubular extraction rate and tubular secretion rate can be derived from the TACs to assess tubular function.
(vi) Modeling techniques: Mathematical models, such as compartmental models and deconvolution techniques, can be applied to the TACs to reconstruct the underlying physiological processes involved in renal function. These models help to quantify and analyze the data in a more detailed manner.
(vii) Clinical interpretation: The derived parameters and modeling results are interpreted in the context of the patient's clinical condition to aid in diagnosis and treatment planning. Abnormalities in renal function parameters can indicate various renal disorders, such as renal artery stenosis, obstruction, or impaired renal function.

Renal function reconstruction and modeling in dynamic scintigraphy play a valuable role in the assessment of renal function and can provide valuable insights for clinicians in the diagnosis and management of renal diseases.

TACs play a critical role in dynamic renal scintigraphy by quantitatively assessing renal function based on tracer kinetics. Traditional TACs are generated automatically by scintigraphy machines using predefined algorithms and standard ROI selection techniques, typically based on radioactive counting. However, these machine-generated TACs may not fully capture the physiological dynamics of renal function due to their dependence on fixed ROI placement and automated signal processing methods.[2] In addition, standard one-compartment models used in renal function modeling assume homogeneous tracer distribution, which may not accurately represent complex renal clearance mechanisms. While alternative models, such as multi-compartment or physiologically based models, offer more detailed representations, they are computationally intensive and not widely implemented in clinical practice. Moreover, manual TAC reconstruction, which can provide a more physiologically relevant representation by incorporating gray-level value measurements, remains underexplored. There is also a lack of studies comparing different ROI selection techniques, such as rectangular versus free-hand approaches, and their impact on TAC accuracy. To address these gaps, this study aims to assess the accuracy of manually reconstructed TACs, validate an empirical mathematical model for renal function evaluation, and explore the influence of ROI selection methods on TAC accuracy.

The main objective of this work is to experimentally reconstruct TACs from clinical dynamic scintigraphy data and compare them with those automatically generated by the scintigraphy machine based on the main kinetic parameters that can be extracted from clinical TACs.[3-5] The second objective is to compare rectangular and free-hand ROI selection methods using six additional cases. The third objective is to evaluate empirical mathematical fitting functions and a one-compartment model used for

the construction of TACs by modeling the physiological processes in the kidneys.

2. Materials and methods

2.1. Dynamic renal scintigraphy

In this work, the GE Discovery NM630 Gamma camera (GE Hualun Medical Systems Co, China was used for imaging data collection and clinical TAC construction. This camera is used in nuclear medicine for many purposes, including dynamic renal scintigraphy. It is a specialized gamma camera designed for high-resolution imaging with enhanced sensitivity and speed. The camera detects the gamma rays emitted by the radiopharmaceutical and creates images that show the distribution and function of the kidneys over time. During dynamic renal scintigraphy with the GE Discovery NM630 Gamma camera, multiple images are taken at different time points after the injection of the radiopharmaceutical. This allows for the assessment of renal blood flow, GFR, renal function, and the detection of any abnormalities such as obstruction or reflux. The dynamic images produced by this technique provide information to healthcare professionals for the diagnosis and management of various kidney disorders, including renal artery stenosis, renal transplant evaluation, and renovascular hypertension. In addition, it can help in the evaluation of renal function before and after interventions such as surgery or renal artery angioplasty.

The data used in this study were collected from patients who underwent dynamic renal scintigraphy over the past 2 years at the Babor Medical Clinic. In compliance with local regulations, data were anonymized by enabling the anonymization option in the DICOM files before extraction. Dynamic renal scintigraphy began immediately after the intravenous injection of TC-99m diethylene triamine penta-acetic acid (DTPA), with the dose based on the patient's weight and other factors, and by considering 12 healthy and pathogenic cases from the Setif region (Algeria) with different sexes and ages. The detectors were positioned in an H-shaped configuration over the abdomen, and the patient was placed in the supine position. Dynamic renal scintigraphy was performed according to standard protocols.[6] In the imaging protocols used in this work, 30 frames were captured during the 1st min, and then 90 frames were captured at a sequence of three frames per minute. The image acquisition process continued for a total duration of 30 min to monitor the tracer uptake, distribution, and clearance in the kidneys. "*Xeleris* GE health care (USA)," was used to automatically generate the clinical TAC, allowing clinicians to select the ROI corresponding to the two kidneys and background on the image sum of all captured frames. It is necessary to ensure that the entire kidney (for functional determination) and the renal pelvis (for pyelocaliceal drainage) are included in the ROI. A larger ROI is preferred over a narrowly surrounding region around the kidney.

From the established TAC, the parameters characterizing the kinetics of renal function that can be assessed are the following:

(i) Split function: It is particularly useful in identifying unilateral changes or differences in renal function and is calculated by generating a TAC that plots the amount of radioactive material in the kidney over time. The split function value is obtained by dividing the counts collected during the uptake phase for each kidney by the sum of the counts from both kidneys. Normal range values of this index are between 42% and 58%.[7-12]

(ii) Relative uptake: The measurement of the radiopharmaceutical's relative uptake is crucial in assessing the specific renal function, which varies depending on the radiopharmaceutical used. When using 99mTc-MAG3 and DTPA, a common approach involves placing an ROI over each kidney and calculating the integrated counts within the renal ROI during specific time intervals (e.g., 1 – 2 min, 1 – 2.5 min, or 2 – 3 mins) after injection. Another method that can be used is the Rutland-Patlak plot.[7-12]

(iii) Time to peak (TTP or T_{max}): It refers to the time it takes for the tracer concentration to reach its highest point or the peak value (maximum concentration in the kidney) when the accumulation trend of the radiopharmaceutical is reversed. In general, for a healthy kidney, TTP values are about 5 min, and the maximum activity at the peak decreases to half the value after 15 min from the injection.[13]

(iv) Clearance time ($T_{1/2}$): It is a quantitative parameter commonly used to describe the rate at which the radiopharmaceutical is cleared from the kidney. It represents the time taken for the radiopharmaceutical activity to decrease by half in the ROI after reaching its peak uptake. This parameter is important in diuretic renography for detecting urinary tract obstruction.[13]

(v) The 30-min min/max ratio: It reflects the time it takes for the radiopharmaceutical to pass through the kidneys. It indicates the amount of residual activity in the cortex. It is calculated by comparing the radioactivity level in the kidneys at 30 min to the peak concentration. This ratio is helpful in diagnosing urinary tract blockages and renovascular hypertension.[13]

(vi) Upslope ratio: It refers to the ratio of the maximum slope of the TAC during the ascending limb to the average slope of the entire curve. This parameter

indicates the rate at which the radiopharmaceutical is taken up by the kidney tissue.

(vii) Downslope ratio: The ratio between the slope of the descending limb of the TAC (representing radiotracer excretion) and the peak activity or uptake slope is used to assess the rate of tracer clearance from the renal parenchyma.

2.2. Manual reconstruction of the TAC using the region of interest selection method

In this work, we proposed a manual method for establishing TACs based on the analysis of scintigraphic images obtained according to clinical protocols and the measurement of gray-level values within specific ROIs corresponding to the kidneys and background. These images were derived from the physical signal (radioactive counting) after undergoing several processing and conversion steps (e.g., amplification, gain, filtering, and analog-to-digital conversion). The procedure, applied to 12 cases, was performed according to the following main steps:

(i) Extraction of patient files, including scintigraphic images, in DICOM format.

(ii) Analyzing of images by micro-DICOM software (v.3.1.1, MicroDicom Ltd, Bulgaria).

(iii) Delineation of the necessary ROIs was performed according to analytic recommendations, ensuring consistent kidney dimensions and coverage across all scintigraphic images (frames). The selection of ROI corresponding to the right and left kidney areas, along with the background on the scintigraphy frames, can be performed using two methods: The free-hand method or the regular shape method. In this work, the regular method was employed using rectangular ROIs (Figure 1).

(iv) Manual construction of TAC from the extracted gray-level values measured on ROIs.

The proposed method for manual TAC reconstruction in dynamic renal scintigraphy relies on analyzing scintigraphic images obtained according to clinical protocols. These images were generated through a sequence of physical and digital processing steps applied to radioactive signals detected by the gamma camera. Below is a detailed breakdown of the steps involved in image formation, processing, and the subsequent TAC reconstruction:

Step#1: The acquisition of physical signal (radioactive counting): The dynamic renal scintigraphy begins with the intravenous injection of a TC-99m DTPA radiopharmaceutical. Once injected into the bloodstream, the tracer is filtered by the kidneys, allowing for an evaluation of renal function through its uptake and clearance. The emitted gamma radiation from the tracer is detected using a gamma camera (GE Discovery NM630), which captures images of the kidneys over time. The imaging protocol employed in this study reportedly included:

(i) 30 frames during the 1st min, allowing an analysis of early tracer uptake.

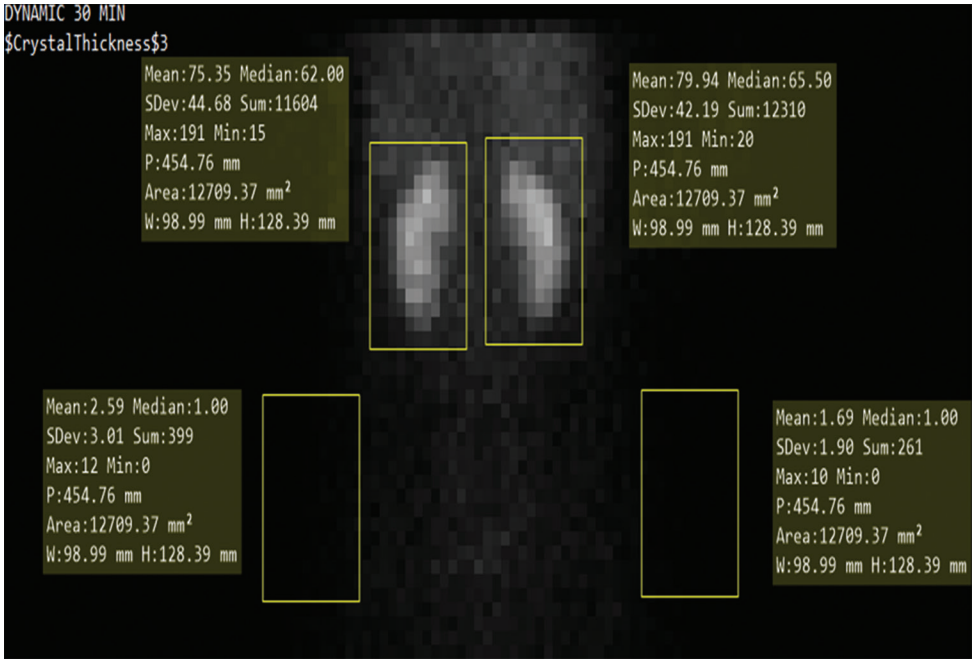

Figure 1. Regular rectangular region of interest selection method used in this study for delineating kidney regions and background areas in scintigraphic images. This method ensures consistency in kidney dimensions and coverage across all scintigraphic frames.

(ii) 90 additional frames at one frame per minute, ensuring a complete observation of renal function over 30 min.

Step#2: The processing and conversion of signals: Since the manually reconstructed TACs are based on gray-level values, these images must undergo several transformation steps before they can be analyzed. The radioactive signals detected by the gamma camera are subjected to various physical and digital processing operations aimed at enhancing accuracy:

(i) Gamma-ray detection: The radiation emitted by the radiopharmaceutical is detected by the gamma camera. It has been noted that this detected signal consists of electrical pulses, which correspond to the intensity of gamma radiation.
(ii) Amplification: To enhance sensitivity, the weak gamma signal is amplified through a photomultiplier tube. This component converts the low-energy gamma photons into stronger electrical signals.
(iii) Gain adjustment: The amplified signal is then subjected to gain correction, a step which is intended to optimize signal detection while reducing unwanted variations. This adjustment ensures that the system maintains an appropriate balance between sensitivity and noise reduction.
(iv) Filtering: Various filtering techniques are applied to refine the detected signal. Energy windowing and scatter correction are commonly utilized to remove background noise and irrelevant signals, thereby improving the reliability of the extracted data.
(v) Analog-to-digital conversion: To allow for further digital analysis, the processed signals are converted into numerical pixel values. This conversion assigns intensity values to pixels in the generated images, enabling subsequent image processing and data extraction.

Step#3: The manual reconstruction of TACs: Once the images are processed, manual TAC reconstruction is performed. The method follows a structured approach:

(i) Extraction of scintigraphic images: The scintigraphic images, stored in DICOM format, are retrieved from the gamma camera system for further analysis.
(ii) Image visualization and ROI selection: The micro-DICOM software (v3.1.1) is employed to display and analyze the extracted images. The ROIs for both kidneys and background areas are then delineated, ensuring that renal function is assessed in a controlled and reproducible manner.
(iii) Methods of ROI selection: Two main approaches for defining the ROIs:
    - Regular shape method (rectangular ROI): This approach, which was implemented in this study, ensures consistency by using a rectangular selection over the kidneys. It is believed to offer improved reproducibility by maintaining standardized ROI dimensions across different frames.
    - Freehand method: Although not applied in this study, this alternative method allows for a more precise delineation of the kidneys' actual shape. While offering greater flexibility, it has been suggested that it may introduce variability depending on operator expertise.
(iv) Extraction of gray-level data: Following ROI selection, gray-level values are extracted from the scintigraphic images. These values reflect the distribution of the radioactive tracer within the kidneys over time.
(v) Construction of TACs: The extracted gray-level data is used to manually reconstruct TACs, which describe the uptake and clearance of the radiopharmaceutical over the 30-min imaging period. The manually generated TACs are then compared with the machine-generated TACs, allowing an evaluation of their accuracy in representing renal function.

2.3. Region of interest selection methods

To study the impact of ROI selection methods in dynamic renal scintigraphy, two selection methods were compared:

(i) Rectangular ROI selection: A fixed, standardized rectangular shape applied to selected data.
(ii) Free-hand ROI selection: A manually drawn contour following the anatomical shape of the kidneys.

The comparison was applied for six additional cases (P1 – P6). The comparison of ROI selection methods was performed to determine whether free-hand ROI selection improves the accuracy of renal function assessment of the considered cases in terms of kinetic parameters.

2.4. TAC modeling using a one-compartment model and fitting function

Most kinetic analyses in dynamic renal scintigraphy rely on mathematical models, typically compartmental models, to study the behavior of a tracer from injection to clearance. These models incorporate an input function that represents the amount of radioactivity injected into the patient. The proposed models take integro-differential forms and are time-dependent. Such modeling can provide information and data on the dynamics of the tracer within the patient and the target organ (the kidney) without the need for experiments or clinical trials. The estimation of the kinetic parameters within the compartmental model is a non-linear regression that uses iterative algorithms, based on the following assumptions:[13]

(i) The measurements are conducted under the condition that physiological processes remain in a steady state throughout the experiment;
(ii) The radioligand used does not significantly affect the physiological or biochemical processes being studied; and
(iii) The homogeneity of the tracer concentration is within each compartment.

Commonly, a compartmental model is defined by a system of differential equations where each equation corresponds to the sum of all transfer rates to and from a specific compartment:

$$\frac{dC_i(t)}{dt} = \sum_{i=1}^{N}\left[k_{ij}C_j(t) - k_{ij}C_i(t)\right]_{i\neq j} \quad \text{(I)}$$

Where $C_i(t)$ is the tracer concentration in compartment i, k_{ij} is the transfer rate constant to compartment i from compartment j, and N is the number of compartments in the model.

In this work, a one-compartment model was used. This model assumes that the system used in this study comprises only one homogenous compartment (Figure 2). After the administration via an extravascular route, the radioactive tracer transfer through the kidney proceeds as follows:[14]

$$\frac{dC_{CE}(t)}{dt} = k_1 C_P(t) - k_2 C_{CE}(t) \quad \text{(II)}$$

Where k_1 is related to the glomerular filtration and equal to the ratio of GFR to the extravascular functional renal cortical volume (GFR/V_{EC}),[15-17] k_2 is related to the urination, C_P is the plasma activity concentration, and C_{EC} is the extravascular functional renal cortical activity concentration.

The solution to the differential equation (Equation II), which describes the variation of activity ($A(t)$) as a function of time (t), is given by the following equation:[14]

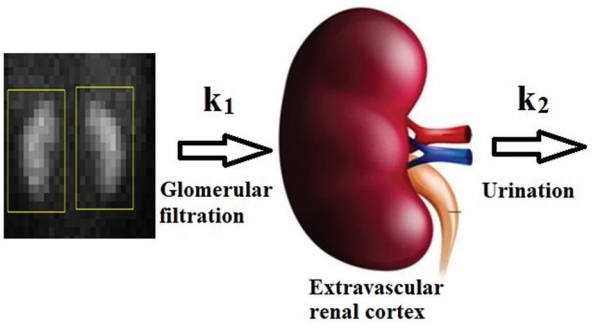

Figure 2. Example of segmentation of the functional renal cortex (left) and schematic representation of the one-compartment tracer kinetic model (right). The one-compartment model describes the uptake and clearance of the radiopharmaceutical tracer in the kidney, with rate constants k_1 (glomerular filtration) and k_2 (urination) representing tracer kinetics.

$$A(t) = A_0(1 - e^{-k_1 \cdot t}) \times e^{-k_2 \cdot t} \quad \text{(III)}$$

In this work, instead of using the analytical solution given by Equation III, an empirical solution was adopted based on imaging data and the manual reconstruction of the TAC. Following multiple trials and with consideration of renal physiology and function, the manually reconstructed TAC was fitted using a suitable mathematical function. This fitting function describes the variation of gray level over time and is presented in Equation IV:

$$GL = \frac{A_0}{(1+\frac{C_e}{t})^{\alpha_e} + (1+\frac{t}{C_s})^{\alpha_s}} \quad \text{(IV)}$$

Where GL is the gray level of a separated frame, A_0 is the activity concentration of the tracer that is injected and metabolized by the kidney, C_e is the perfusion time constant, α_e is a weighting factor of the perfusion phase, C_s is a time constant in the secretion-drainage phase (urination), α_s is a weighting factor related to the secretion-drainage phase, and t is the time variable.

3. Results

Figure 3 demonstrates an example of clinical (machine) and manually reconstructed TACs of Case 1.

Figure 4 shows the TAC modeling for Case 1 using the mathematical fitting function (Equation IV) based on the one-compartment model.

Table 1 compares the kinetic parameters of the renal function automatically generated by the scintigraphy machine's algorithm with those manually extracted using the proposed model.

Manually reconstructed renal TACs were found to be dependent on the ROI selection methods. While the results obtained using the manual method were accurate and of good quality, the free-hand selection method is believed to offer better results, particularly for mathematical modeling and data fitting. This approach may enhance the accuracy of the main kinetic parameters extracted from the data. Moreover, the renal function curves established manually using gray-level values from individual scintigraphic images exhibited better dynamic behavior than those from the machine (automatic), which are based on radioactive counting. This difference is due to the gain adjustment between radioactive counts and gray level during the analog-to-digital conversion phase. In addition, the processing of the physical signals (radioactive counting) also plays a critical role in influencing the final TAC output.

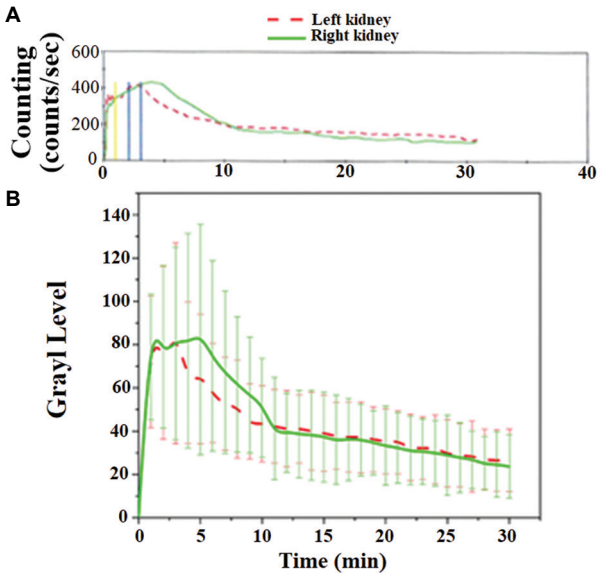

Figure 3. Comparison of TACs for Case 1. (A) TAC was generated automatically by the scintigraphy machine. (B) TAC was reconstructed manually from processed dynamic renal scintigraphic images using the proposed regular rectangular region of interest selection method. The manually reconstructed TAC exhibits a more detailed dynamic behavior than the machine-generated TAC.
Abbreviation: TACs: Time-activity curves.

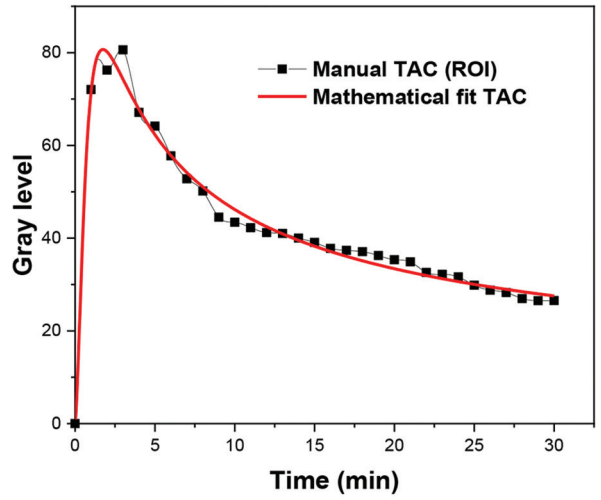

Figure 4. Mathematical modeling of the manually reconstructed TAC for the healthy kidney in Case 1. The experimental data points extracted from scintigraphic images (black circles) were fitted using the proposed empirical fitting function based on a one-compartment model with additional adjusting parameters. The fitted curve (solid red line) closely follows the manual TAC, demonstrating the accuracy of the proposed model.
Abbreviation: TAC: Time-activity curve.

Table 2 presents a numerical comparison of the kinetic parameters extracted using both ROI selection methods (rectangular and free-hand).

The statistical analysis of the results in Table 2 is summarized in Table 3.

The results and statistical analyses demonstrate that the free-hand ROI selection method yields significantly lower T_{max} values, indicating a more precise capture of peak tracer uptake. This method also exhibits a significantly shorter tracer elimination time, likely due to better exclusion of background noise. Regarding the 30-min min/max ratio, the free-hand ROI selection method shows a significantly lower residual activity, allowing for more accurate isolation of renal function. Overall, the free-hand ROI selection method provides physiologically more accurate TACs by closely contouring kidney anatomy and minimizing background activity. In contrast, the rectangular ROI selection method provides consistency across cases but may include non-kidney regions, which can lead to slightly overestimated retention values.

To evaluate the effectiveness and accuracy of the proposed fitting function and empirical model, standard goodness-of-fit metrics were used, including the correlation factor (R^2), adjusted R^2, and reduced χ^2. For Case 1, Table 4 indicates a high-quality fit, with R^2 and adjusted-R^2 values close to 1, and a low reduced χ^2, confirming the model's robustness. The fitting parameters, particularly C_s and α_s, reflect the pathological status of the left and right kidneys. Similar results were observed across all other cases.

The proposed clinical data fitting function proved suitable for the extraction of key kinetic parameters of renal function. It can be applied in any simulation aimed at evaluating new radiopharmaceuticals (radiotracers) for use in dynamic renal scintigraphy, as well as for other tasks of interest.

4. Discussion

The findings of this study underscore the significant advantages of manual reconstruction and mathematical modeling of TACs in dynamic renal scintigraphy over the automatic algorithms of standard imaging systems. By integrating manual ROI selection with an empirical mathematical fitting function, this study successfully reconstructed TACs with greater accuracy and physiological relevance.[18]

The manually reconstructed TACs demonstrated improved dynamic behavior compared to the machine-generated TACs. This superiority can be attributed to the differences in data processing techniques. While machine-generated TACs rely on raw radioactive counts, the manual method incorporates gray-level values that undergo additional processing steps, such as analog-to-digital conversion and filtering. This approach likely enhances

Table 1. Comparison between the main kinetic parameters obtained automatically (clinical) and those manually extracted through mathematical modeling of the 12 time-activity curves

Kinetic parameters	Right kidney		Left kidney	
	Automatic data	Manual data	Automatic data	Manual data
Case 1				
T_{max} (min)	4.05	4.26	2.71	2.88
$T_{1/2}$ (min)	5.67	6.18	7.00	6.70
30-min min/max ratio	0.26	0.28	0.31	0.32
Case 2				
T_{max} (min)	1.01	1.43	3.34	3.35
$T_{1/2}$ (min)	10.67	12.79	15.00	15.65
30-min min/max ratio	0.47	0.39	0.42	0.37
Case 3				
T_{max} (min)	4.00	4.20	4.10	4.18
$T_{1/2}$ (min)	9.50	8.70	9.20	8.60
30-min min/max ratio	0.30	0.28	0.29	0.30
Case 4				
T_{max} (min)	3.50	3.76	3.60	3.88
$T_{1/2}$ (min)	10.00	10.18	10.20	9.80
30-min min/max ratio	0.28	0.30	0.30	0.31
Case 5				
T_{max} (min)	4.50	4.66	4.40	4.32
$T_{1/2}$ (min)	8.50	8.25	7.50	7.70
30-min min/max ratio	0.25	0.26	0.26	0.28
Case 6				
T_{max} (min)	3.50	3.83	1.75	1.85
$T_{1/2}$ (min)	11.00	10.54	12.00	12.78
30-min min/max ratio	0.32	0.31	0.34	0.33
Case 7				
T_{max} (min)	4.20	4.28	4.10	4.07
$T_{1/2}$ (min)	9.00	8.95	8.80	8.70
30-min min/max ratio	0.27	0.28	0.28	0.27
Case 8				
T_{max} (min)	7.50	7.76	6.75	6.90
$T_{1/2}$ (min)	25.05	26.30	24.30	26.65
30-min min/max ratio	0.70	0.78	0.65	0.68
Case 9				
T_{max} (min)	4.70	4.90	8.05	8.26
$T_{1/2}$ (min)	8.25	9.70	30.00	29.12
30-min min/max ratio	0.35	0.37	0.75	0.78
Case 10				
T_{max} (min)	4.50	4.25	4.71	4.08
$T_{1/2}$ (min)	8.00	7.81	7.50	7.70
30-min min/max ratio	0.25	0.26	0.26	0.27

(*Cont'd...*)

Table 1. (*Continued*)

Kinetic parameters	Right kidney		Left kidney	
	Automatic data	Manual data	Automatic data	Manual data
Case 11				
T_{max} (min)	4.15	4.05	4.71	4.32
$T_{1/2}$ (min)	5.75	6.60	7.00	7.14
30-min min/max ratio	0.22	0.28	0.30	0.31
Case 12				
T_{max} (min)	4.15	4.35	9.00	9.22
$T_{1/2}$ (min)	6.20	6.45	35.00	36.20
30-min min/max ratio	0.26	0.27	0.45	0.48

Table 2. Comparison of the kinetic parameters between the two region-of-interest selection methods

Case	Kidney	ROI selection method	T_{max} (min)	$T_{1/2}$ (min)	30-min min/max ratio
P1	Left	Rectangular	4.2	8.5	0.32
		Free-hand	4.0	7.9	0.28
P2	Right	Rectangular	3.8	9.2	0.35
		Free-hand	3.5	8.7	0.30
P3	Left	Rectangular	4.5	7.8	0.29
		Free-hand	4.3	7.4	0.26
P4	Right	Rectangular	5.1	10.1	0.38
		Free-hand	4.8	9.6	0.33
P5	Left	Rectangular	4.0	8.9	0.31
		Free-hand	3.8	8.2	0.27
P6	Right	Rectangular	3.7	9.5	0.34
		Free-hand	3.4	9.1	0.29

Table 3. Statistical analysis of the comparison between the two ROI selection methods

Statistical parameters	ROI selection method	
	Rectangular	Free-hand
Mean and standard deviation		
T_{max} (min)	4.22±0.52	4.00±0.49
$T_{1/2}$ (min)	8.99±0.83	8.32±0.74
30-min min/max ratio	0.33±0.03	0.29±0.02
Paired t-test results (rectangular vs. free-hand)		
T_{max}	p=0.035*	
$T_{1/2}$	p=0.041*	
30-min min/max ratio	p=0.029*	
Correlation analysis (R^2 values between the TACs of both methods)	R^2=0.94	

Note: *p<0.05.
Abbreviations: TAC: Time-activity curve; ROI: Region-of-interest.

Table 4. Fitting function and mathematical model parameters of Case 1

Fitting function parameters	Left kidney	Right kidney
A_0	5,687	200,181
C_e	0.98	3.35
α_e	1.90	1.45
C_s	4.91	0.0011
α_s	0.48	0.88
Reduced χ^2	4.77	13.95
R^2	0.98	0.97
R^2 adjusted	0.98	0.96

Notes: A_0 indicates the activity concentration of the tracer that is injected and metabolized by the kidney; C_e indicates the perfusion time constant; α_e indicates a weighting factor of the perfusion phase; C_s indicates a time constant in the secretion-drainage phase (urination); α_s indicates a weighting factor related to the secretion-drainage phase, and t is the time variable.

sensitivity to subtle physiological variations, reflected in the closer alignment of manually derived kinetic parameters (e.g., T_{max} and $T_{1/2}$) with expected renal physiology.[19]

The comparative analysis of the kinetic parameters, including T_{max}, $T_{1/2}$, and the 30-min min/max ratio, revealed small yet significant differences between manual and automatic methods. For example, in all analyzed cases, manual reconstruction resulted in slightly higher T_{max} values, reflecting a potentially more accurate depiction of tracer dynamics. Similarly, the improved correlation factors (R^2 and reduced χ^2 values) for the mathematical fitting function indicate the robustness of the proposed model in capturing physiological processes.

The proposed empirical mathematical model demonstrated excellent accuracy in modeling TACs, as evidenced by high R^2 and adjusted R^2 values. Parameters such as *Cs* and *αs*, derived from the fitting function, provided insights into the pathological status of the kidneys. This adaptability of the model highlights its potential utility in clinical and research settings, including the evaluation of new radiopharmaceuticals and the investigation of renal pathophysiology.

One notable limitation of this study is the dependency of manual TAC reconstruction on the ROI selection method. While the rectangular ROI selection method used here ensured consistency, a free-hand approach may offer even greater accuracy by better conforming to kidney shapes. Future studies should explore the impact of different ROI selection methods on the accuracy of TACs and kinetic parameters. In addition, extending this methodology to a larger cohort with diverse renal pathologies could validate its generalizability and clinical applicability. If accuracy is prioritized, the free-hand ROI selection method is preferable. However, if standardization and reproducibility are the main concerns, the rectangular ROI selection method may still be useful. The presented comparison demonstrates how the choice of ROI selection method can influence kinetic parameters in renal scintigraphy.

The proposed manual method offers an alternative approach to TAC reconstruction by leveraging gray-level values rather than direct radioactive counting. It involves several crucial steps, including image acquisition, processing, ROI selection, data extraction, and TAC reconstruction. While this method enhances dynamic accuracy, future studies could focus on minimizing inter-operator variability and evaluating its applicability across diverse renal conditions and imaging systems to improve generalizability to complex cases and pathologies.

The findings of this study suggest that manual reconstruction and modeling of TACs could enhance the diagnostic accuracy of dynamic renal scintigraphy, particularly in complex or borderline cases. The ability to extract more physiologically relevant parameters could improve the detection of subtle renal dysfunctions and provide a more detailed assessment for treatment planning. In clinical practice, this can be particularly advantageous in detecting early-stage renal dysfunction, assessing post-transplant renal function, or identifying subtle abnormalities that might be overlooked by machine-generated TACs.

5. Conclusion

This study demonstrates the effectiveness of manual reconstruction and empirical modeling of TACs in dynamic renal scintigraphy. The manually established TACs provide more physiologically relevant insights compared to those automatically generated by scintigraphy machines. By leveraging gray-level data and a one-compartment model, the proposed approach achieved superior dynamic behavior and higher accuracy in extracting key kinetic parameters, such as T_{max} and $T_{1/2}$. The fitting function developed in this work proved robust, with excellent correlation coefficients and goodness-of-fit metrics. These results highlight the potential of manual TAC modeling in improving diagnostic accuracy and exploring renal pathophysiology. Moreover, the method offers a valuable framework for evaluating new radiopharmaceuticals and advancing clinical applications. However, future work should address the limitations of ROI selection methods and validate the findings across larger patient cohorts. Overall, this study advances the understanding of renal function reconstruction and modeling, paving the path for enhanced clinical and research applications in nuclear medicine.

Acknowledgments

None.

Funding

None.

Conflict of interest

The authors declare no conflicts of interest.

Author contributions

Conceptualization: Faycal Kharfi
Investigation: All authors
Methodology: Faycal Kharfi
Writing – original draft: Faycal Kharfi
Writing – review & editing: Faycal Kharfi

Ethics approval and consent to participate

Patient data were used anonymously in accordance with local ethical guidelines. The study does not involve clinical trials and does not require informed consent.

Consent for publication

Patient data were used anonymously and do not require consent for publication.

Availability of data

The data are not publicly available.

References

1. Alsabea H. Type of renal scintigraphy. *J Nucl Med Radiat Ther*. 2017;8(6):347.

   doi: 10.4172/2155-9619.1000347

2. Esser JP. *Dynamic Renal Scintigraphy (Part I)*. Amersfoort: Meander Medical Centre; 2014.

3. Tyagi N, Pandey A, Parihar A, *et al*. Analysis of the efficacy of elastography in comparison with dynamic renal nuclear scintigraphy in the evaluation of unilateral pelvie-ureteric junction obstruction. *J Pediatr Surg*. 2024;59:605-609.

   doi: 10.1016/j.jpedsurg.2023.11.017

4. Volkan-Salanci B, Erbas B. Diuretic renal scintigraphy in adults: Practical aspects and reporting. *Semin Nucl Med*. 2021;52:445-452.

   doi: 10.1053/j.semnuclmed.2021.12.006

5. Nilsson JN, Elovsson R, Thor D, Calissendorff J, Ardenfors O. Radioiodine treatment outcome by dosimetric parameters and renal function in hyperthyroidism. *Thyroid Res*. 2022;15:8.

   doi: 10.1186/s13044-022-00126-4

6. François H, Richardson A, Boubaker A, *et al. Dynamic Renal Imaging in Obstructive Renal Pathology a Technologist's Guide*. Austria: European Association Nuclear Medicine; 2009. p. 1-23.

   doi: 10.52717/NAYK4703

7. Grzegorz Filipczak K, Cichocki P, Kusmierek J, Plachcinska A. Kidney efficiency index - quantitative parameter of a dynamic renal scintigraphy. I. Theory and preliminary verification. *Nucl Med Rev*. 2020;23(2):78-83.

   doi: 10.5603/NMR.2020.0025

8. Wu R, Huang D, Wang Z, *et al*. The Application of Renal Dynamic Imaging in Measuring Renal Function of En-Bloc Pediatric Kidneys Transplanted into Recipients. In: Liu C, editors. *Proceedings of the 23rd Pacific Basin Nuclear Conference. Springer Proceedings in Physics*. Vol. 3. Singapore: Springer; 2023. 233-245.

   doi: 10.1007/978-981-19-8899-8-24

9. Grilo N, Schurch B. Renal Function Evaluation. In: Liao L, Madersbacher H, editors. *Handbook of Neurourology*. Singapore: Springer; 2023.

   doi: 10.1007/978-981-99-1659-7-21

10. Civan C, Simsek DH, Kiran MY, *et al*. Comparison of 2D planar and 3D volumetric methods for estimation of split renal function by 99mTc-DMSA scintigraphy. *Phys Med*. 2022;95:83-88.

    doi: 10.1016/j.ejmp.2022.01.010

11. Reichkendler MH, Berg RMG, De Nijs R, Nørgaard H, Schmidt IM, Borgwardt L. Planar scan vs. SPECT/low-dose CT for estimating split renal function by ^{99m}Tc-DMSA scintigraphy in children. *Eur J Nucl Med Mol Imaging*. 2020;47(3):729-733.

    doi: 10.1007/s00259-019-04575-2

12. Orrico M, Cosma L, Ricci M, *et al*. Early renal function alterations in renal branches vs. Renal fenestrations - a dynamic scintigraphy based prospective study. *Eur J Vasc Endovasc Surg*. 2020;60(3):395-401.

    doi: 10.1016/j.ejvs.2020.05.023

13. Taylor AT. Radionuclides in nephrourology, part 1: Radiopharmaceuticals, quality control, and quantitative indices. *J Nucl Med*. 2014;55(4):608-615.

    doi: 10.2967/jnumed.113.133447

14. Kersting D, Sraieb M, Seifert R, *et al.* First experiences with dynamic renal [^{68}]Ga]Ga-DOTA PET/CT: A comparison to renal scintigraphy and compartmental modelling to non-invasively estimate the glomerular filtration rate. *Eur J Nucl Med Mol Imaging.* 2022;49:3373-3386.

    doi: 10.1007/s00259-022-05781-1

15. Murray AW, Barnfield MC, Waller ML, Telford T, Peters AM. Assessment of glomerular filtration rate measurement with plasma sampling: A technical review. *J Nucl Med Technol.* 2013;41(2):67-75.

    doi: 10.2967/jnmt.113.121004

16. Rahimi A, Hosntalab M, Babapour Mofrad F, Amoui M, Bagci U. An automatic segmentation framework for computer-assisted renal scintigraphy procedure. *Med Biol Eng Comput*. 2023;61:285-295.

    doi: 10.1007/s11517-022-02717-7

17. Aggarwal P, Gunasekaran V, Gowtham M, *et al.* Assessment of post-pyeloplasty renal drainage in antenatally detected hydronephrosis by $^{99]m}$Tc-L, L-Ethylenedicysteine renal scintigraphy: The importance of delayed imaging. *Ann Nucl Med*. 2024;39:266-272.

    doi: 10.1007/s12149-024-01994-6

18. Zheng X, Wei W, Huang Q, Song S, Huang G. Automated

region of interest detection method in scintigraphic glomerular filtration rate estimation. *IEEE J Biomed Health Informatics*. 2019;23(2):787-794.

doi: 10.1109/JBHI.2018.2845879

19. Pi Y, Zhao Z, Yang P, *et al*. Deep regression using ^{99m}Tc-DTPA dynamic renal imaging for automatic calculation of the glomerular filtration rate. *Eur Radiol*. 2023;33:34-42.

doi: 10.1007/s00330-022-08970-6